This means that

The L-C Oscillator Circuit

IVOR CATT

Abstract—The traditional differential equation approach to the circuit assumes that the components are lumped. However, work on high-speed logic has led to a new view which recognizes that the L and C are distributed in space.

Manuscript received January 11, 1983; revised March 11, 1983.
The author is with Watford College, Watford, England.

When a charged capacitor is connected to an inductor, the conventional analysis is to equate the voltage across the capacitor with the voltage across the inductor

$$v = \frac{1}{C}\int i\,dt = -L\frac{di}{dt}.$$

Differentiating, we get

$$\frac{d^2 i}{dt^2} = -\frac{i}{LC}.$$

This is then recognized as having as a solution simple harmonic motion, $v = v_0 \sin \omega t$, where $\omega^2 = 1/LC$.

The traditional analysis assumes that when current is switched into the inductor, it appears instantaneously at all points in the inductor; the use of the single, lumped quantity L implies this. Similarly, it is assumed that the electric charge density at all points in the capacitor is the same; that there are no transient effects such that the charge density is greater in certain regions of the capacitor plates.

Work on high-speed logic systems has led to a reappraisal of the conventional analysis, particularly insofar as it bears on the choice of type and value of decoupling capacitor for logic power supplies.

The rest of this letter outlines a new approach to the subject.

Consider a capacitor (or open-circuit transmission line) which is connected to a single-turn inductor (or short-circuited transmission line). The initial state could be that the capacitor was charged to a voltage v and then connected to the inductor by closing the switches. However, other initial states could be proposed.

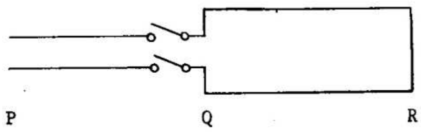

In general, the following coefficients apply when signals reflect or pass through discontinuities in the circuit.

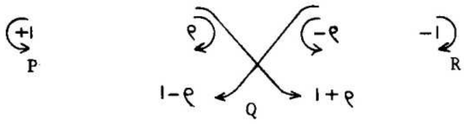

If at a certain time the signal in the capacitor PQ has an amplitude v_{x-1} and the signal amplitude in the inductor L is y, then the following sequence will occur.

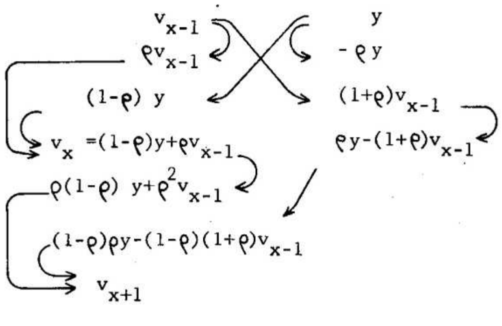

The sequence above is explained as follows. v_{x-1}, coming from the left to Q, breaks up into a reflected signal ρv_{x-1} and a forward signal $(1+\rho)\,v_{x-1}$ because the two relevant coefficients are ρ and $(1+\rho)$. At the same time, the signal y, coming from the right towards Q, breaks up into a forward going $(1-\rho)\,y$ and a reflecting $-\rho y$, because the relevant coefficients are $(1-\rho)$ and $(-\rho)$. $(1-\rho)\,y$, traveling to the left from Q, combines with the leftwards traveling ρv_{x-1}. When they reach the open circuit at P, where the reflection coefficient is $+1$, they reflect back towards Q. The value of this signal is now v_x, the next in the sequence, and we have calculated it to equal $(1-\rho)\,y + \rho v_{x-1}$. Similar arguments explain all other amplitudes in the sequence.

The bottom line of the sequence gives us the value of v_{x+1} in terms of y and v_{x-1}. If we add v_{x-1} to this value of v_{x+1}, we get

0018-9219/83/0600-0772$01.00

$$v_{x+1} + v_{x-1} = 2\rho(1-\rho)y + [1-(1-\rho^2)+\rho^2]\, v_{x-1}$$
$$= 2\rho(1-\rho)y + 2\rho^2 v_{x-1}$$
$$= 2\rho[(1-\rho)y + \rho v_{x-1}].$$

But the middle line of the sequence tells us that

$$v_x = (1-\rho)y + \rho v_{x-1}.$$

Therefore,

$$v_x = \frac{v_{x+1} + v_{x-1}}{2\rho}.$$

$2v_x$, $2v_{x+1}$, $2v_{x+2}$, etc., is a sequence of amplitudes seen in the capacitor, and they obey the above formula. Now since

$$\sin a = \frac{\sin(a+\delta a) + \sin(a-\delta a)}{2\cos\delta a}$$

we can see that one possibility is that the sequence in v_x represents a series of steps which approximate to a sine wave.

The conclusion is that one waveform which can be supported by an L-C circuit is a sine wave, where C is an open-circuit transmission line and the L is a short-circuited transmission line. The larger the value of ρ (i.e., the bigger the discrepancy between Z_{0C} and Z_{0L}, or to put it another way, the more capacitive the capacitor and/or the more inductive the inductor), the smaller is the forward flow of current each time across the central node at Q between the C and the L. This means that there is more time between maxima in the voltage level in C, and a lower "resonant frequency."

The two-turn inductor problem will probably be solved along the lines indicated in [1], [2].

References

[1] I. Catt, *Electromagnetic Theory.*, 17 King Harry Lane, St. Albans, England: C.A.M. Publishing, 1980, p. 223.

[2] ——, "Crosstalk (noise) in digital systems," *IEEE Trans. Electron. Comput.*, vol. EC-16, pp. 743-763, Dec. 1967.

Distribution of Natural Frequencies in Electrical Ladder Networks

ANTONIO LLORIS, A. PRIETO, AND J. SANCHEZ-DEHESA

Abstract—**The evolution of the distribution of natural frequencies in electrical ladder networks composed by the iteration of the same elemental structure, as the number of sections increase, is analyzed. These networks are seen as a large-scale many-body system. Several collective properties of the spectrum; namely, the eight first moments of the density of natural frequencies, the skewness, and the excess; are explicitly calculated. Different cases of transmission lines represented by ladder networks are considered.**

Introduction

The Kirchhoff's laws of meshes and nodes for a linear, time-invariant electric network with independent voltage and current sources, with $m+1$ meshes and n nodes, are [1]

$$Z_m(s)\cdot I_m(s) = E(s) \qquad \text{(meshes)} \tag{1}$$

$$Y_n(s)\cdot V_n(s) = J(s) \qquad \text{(nodes)} \tag{2}$$

$Z_m(s)$ and $Y_n(s)$ being the impedance and admittance matrices, respectively. The zeros of the determinant of either these matrices are called [2] natural frequencies of the networks, giving very interesting information about the behavior of the network [2]-[8]. These natural frequencies may be obtained from the state equations [1]

Manuscript received October 5, 1982.

The authors are with the Facultad de Ciencias (Fisicas), University of Granada, Granada, Spain.

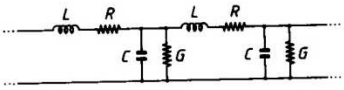

Fig. 1. Equivalent circuit for a transmission line.

$$\frac{d}{dt}X = A\cdot X + B\cdot e \tag{3}$$

$$W = C\cdot X + D\cdot e + E\cdot\frac{de}{dt} \tag{4}$$

where X, e, and W are, respectively, the state, excitation, and output vectors. The natural frequencies of the networks are the eigenvalues of the matrix A [9].

For electrical ladder networks, the A matrix may be tridiagonal if branch currents and node voltages are selected as state variables [10], [11]. Besides, using this type of networks, transmission lines may be represented as a series connection of infinitesimal sections as that given in Fig. 1. This representation is better when more sections are considered, but then the dimension of A and the number of natural frequencies also increases. In this case, the network may be considered as a large-scale many-body system. The number of natural frequencies is very high, so, from a physical point of view, it is more important to know the collective properties of the spectrum than the individual values of the natural frequencies. Our goal is to study the distribution of natural frequencies in electrical ladder networks composed by a repetition of the same elemental structure, when the number of sections increases indefinitely. In this way, standard techniques applied in other fields of physics [12], are used in the circuit theory.

Collective Parameters of the Circuit

To characterize the collective properties of the spectrum, we shall use the moments μ_r, $r = 1, 2, \cdots, N$, which refer to the centroid M of the distribution, defined [13] as

$$\mu_r = \frac{1}{N}\sum_{i=1}^{N}(\lambda_i - M)^r \tag{5}$$

where

$$M = \frac{1}{N}\sum_{i=1}^{N}\lambda_i \tag{6}$$

N being the number of natural frequencies and λ_i these natural frequencies.

Some distributions of frequencies (like the Gaussian, for instance) are well characterized with only the low-order moments. Also, the skewness γ_1 and the excess or kurtosis γ_2 defined [13] as

$$\gamma_1 = \frac{\mu_3}{\mu_2^{3/2}}$$

$$\gamma_2 = \frac{\mu_4}{\mu_2^2} - 3 \tag{7}$$

will be used in the characterization. The skewness gives a measure of the symmetry of the distribution. The excess gives a degree of flattening of the density curve near its centroid.

To obtain these parameters and to analyze their evolution as the number of sections in the ladder increases, a Fortran program has been written. This program considers iteratively a different number of sections and, in each iteration, the matrix A, its eigenvalues, the eight first moments, the skewness, and the excess of the distribution are obtained. The eigenvalues result from a Fortran routine implemented by IMSL [14] using the TQL2 algorithm [15]; this routine also obtains the index of performance designed by EISPACK [14]. With this index, the routine works very well for our problems.

Results and Conclusions

Some ladder networks have been analyzed with our program. We shall mention the following four, all of them corresponding to transmission lines:

0018-9219/83/0600-0773$01.00 © 1983 IEEE

M' is the number of tap weights of transversal in-phase and quadrature bandpass filters which are required for generating the complex input signal of the passband complex equalizer. The convergence speed of this structure can be improved significantly by self-orthogonalization of weight adjustment in the frequency domain as studied by Lee and Un [3].

References

[1] S. Qureshi, "Adaptive equalization," *Proc. IEEE*, vol. 72, pp. 1349–1387, Sept. 1985.
[2] K. H. Mueller and J. J. Werner, "A hardware efficient passband equalizer structure for data transmission," *IEEE Trans. Commun.*, vol. COM-30, pp. 538–541, Mar. 1982.
[3] J. C. Lee and C. K. Un, "Block realization of multirate adaptive digital filters," *IEEE Trans. Acoust., Speech, Signal Processing*, vol. ASSP-34, pp. 105–117, Feb. 1986.
[4] M. S. Sabri and W. Steenaart, "Discrete Hilbert transform filtering," *IEEE Trans. Acoust., Speech, Signal Processing*, vol. ASSP-25, pp. 452–454, Oct. 1977.
[5] A. V. Oppenheim and R. W. Schafer, *Digital Signal Processing*. Englewood Cliffs, NJ: Prentice-Hall, 1975.
[6] J. C. Lee and C. K. Un, "Performance of transform-domain LMS adaptive digital filters," *IEEE Trans. Acoust., Speech, Signal Processing*, vol. ASSP-34, pp. 499–510, June 1986.

The Inductor as a Transmission Line

MICHAEL S. GIBSON AND IVOR CATT

Research into the interconnection of high-speed logic causes us to re-evaluate and modify the traditional view of circuit components like inductors, and to realize that they are not lumped but are distributed in space.

The inductor is a time-delay and energy trap. A voltage step enters and travels back and forth through the device, with gradual trapping of energy inside. The time taken for the energy leaving the inductor to rise to equal the amount entering is dependent on the mismatch between the characteristic impedances and also the time delay involved in traversing the device. If the mismatch is great, less energy enters or leaves per round trip, so the time taken for the equality of energies is longer and therefore the inductance is greater.

The single-turn inductor is a transmission line with an increase in characteristic impedance followed by a short circuit [1]. This letter discusses the two-turn inductor, Fig. 1.

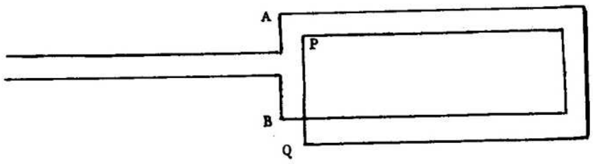

Fig. 1.

When a wavefront traveling down an infinitely long cable reaches AB, it breaks up into three parts; a reflection v_{RC} back up the cable and two transmitted parts. The transmitted parts are the even and odd modes of propagation [2]. The voltages and currents on lines AB and PQ are

$$v_{AB} = v_e + v_o \tag{1}$$

$$i_{AB} = i_e + i_o \tag{2}$$

$$v_{PQ} = v_e - v_o \tag{3}$$

$$i_{PQ} = i_e - i_o. \tag{4}$$

The line PQ has a short which clamps its voltage to zero.

$$v_{PQ} = 0 \tag{5}$$

therefore

$$v_e = v_0. \tag{6}$$

Using basic transmission line theory, (1)–(4) can be solved, yielding

$$T_{ce} = \frac{2}{(2 + R_e + R_o)} \tag{7}$$

$$T_{co} = \frac{2}{(2 + R_e + R_o)} \tag{8}$$

$$R_c = \frac{(2 - R_e - R_o)}{(2 + R_e + R_o)} \tag{9}$$

where

$$R_e = \frac{Z_{cable}}{Z_{even}}$$

$$R_o = \frac{Z_{cable}}{Z_{odd}}$$

T_{ce} means the transmitted voltage from the cable to even mode and R_c is the reflected part from the junction back into the cable. By repeating terminal conditions for the inductor to cable direction, we get

$$T_{ec} = \frac{4R_e}{(2 + R_e + R_o)} \tag{10}$$

$$T_{oc} = \frac{4R_o}{(2 + R_e + R_o)} \tag{11}$$

$$R_{eo} = \frac{2R_e}{(2 + R_e + R_o)} \tag{12}$$

$$R_{ee} = \frac{(-2 + R_e - R_o)}{(2 + R_e + R_o)} \tag{13}$$

$$R_{oo} = \frac{(-2 - R_e + R_o)}{(2 + R_e + R_o)} \tag{14}$$

$$R_{oe} = \frac{2R_o}{(2 + R_e + R_o)}. \tag{15}$$

The far end of the inductor requires special interpretation which eliminates some mathematics. Understanding the meaning of even- and odd-mode propagation given in the 1967 paper [2], one can see that the odd mode is terminated by an open circuit and the even mode by a short circuit. Since the incident voltages are already in the correct modes and each mode is individually terminated, there will be no transfer between even and odd mode at the far end of the inductor. The odd mode is reflected positively and the even mode is simply inverted.

A computer simulation of the two-turn inductor was performed with the following results, shown in Fig. 2.

The graphs show the total voltage on the feeder cable. The damped oscillation is due to the continuous inversion of the even mode at the far end of the inductor.

The time constant, the time for the voltage in the inductor to fall to e^{-1} of maximum, is $\tau = L/R$, where R is the characteristic impedance of the cable Z_c. N is the number of iterations of the program, or traverses of the inductor, needed to reach τ. So the inductance is $L = NTZ_c$, where T is the time taken to traverse the inductor once.

On the graph (Fig. 2), the quadrupling of the inductance from a one-turn inductor to a two-turn inductor is shown. The increase results from the difference in the characteristic impedance of the

Manuscript received September 9, 1986; revised November 25, 1986.
The authors are severally with Odessa Engineering, P. O. Box 26537, Austin, TX 78755, USA, and C. A. M., P.O. Box 99, St. Albans, U.K.
IEEE Log Number 8714162.

0018-9219/87/0600-0849$01.00 © 1987 IEEE

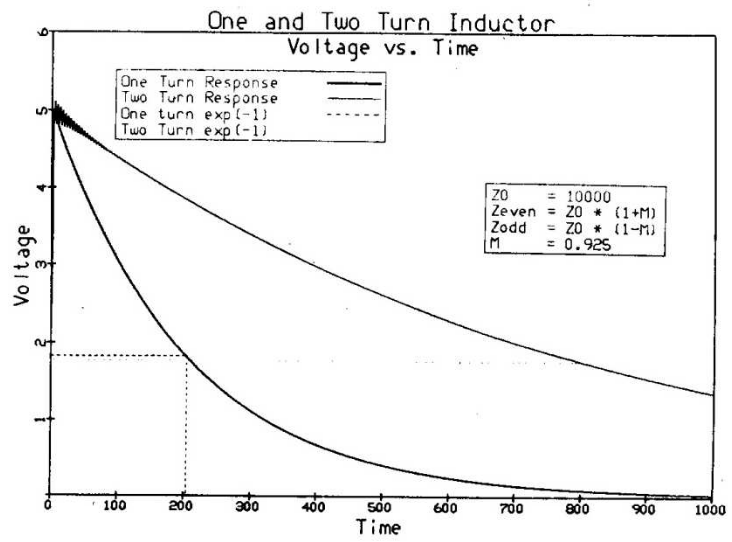

Fig. 2.

even and odd modes. At low mismatches of even and odd (when they are approximately equal), the inductance is only twice that of a one-turn inductor of the same length since the lines are uncoupled. In this case, the two-turn inductor behaves like a single turn of twice the length. But at high mismatches between even and odd modes, that is, when the lines are brought together, the lines are tightly coupled and the modes trapped. This trapping of the modes increases the time taken to reach the steady state (a short circuit), and is detected as an increase in inductance.

References

[1] I. Catt, "The *L-C* oscillator circuit," *Proc. IEEE*, vol. 71, pp. 772–773, June 1983.
[2] —, "Crosstalk (noise) in digital systems," *IEEE Trans. Electron. Comput.*, vol. EC-16, pp. 743–763, Dec. 1967.

Dependence of Process Parameters on Planarization Isolation and Etching of Sloped Vias in Polyimides for GaAs ICs

J. K. SINGH, A. ROYBARDHAN, H. S. KOTHARI, B. R. SINGH, AND W. S. KHOKLE

The effect of imidization condition for realizing sloped vias in polyimide film using positive resist as an etch mask has been investigated. Using chemical etching techniques, vias of tapered angles ranging from 45° to 60° has been obtained for 80-percent imidization of the polyimide film. Results on optimum process conditions for obtaining dielectric breakdown strength of 2MV/cm and degree of planarization of about 58 percent have also been included.

Introduction

Development of a successful multilevel metal interconnect process requires a dielectric layer with excellent insulating property, good degree of planarization, and fine-line patterning ability with sloped vias. Polyimides, a new class of organic dielectric material, possess all the above properties with some additional features such as ease in realization, radiation hardness, and low-temperature process compatibility which makes it highly suitable for GaAs ICs [1]–[9]. Till todate no published data are available on the effect of process parameter on etching of sloped vias in polyimides using chemical etching technique. Recently, Harada *et al.* [1] used hydrazine hydrate and dimethylamine as chemical etchants for polyimide using negative resist as an etch mask. But we found it highly unsuitable for GaAs device fabrication which normally uses a lift-off process and positive resist as an etch mask. Yen [2] used positive resist developer as an alternative etchant for polyimide at the cost of overdeveloping the positive resist, resulting in dimensional losses.

In this letter, optimum process condition for realizing sloped vias in polyimide using chemical etching has been presented. Results on dielectric breakdown strength and degree of planarization for different polyimide deposition conditions are also included.

Manuscript received August 5, 1986; revised September 25, 1986.
The authors are with the Central Electronics Engineering Research Institute, Semiconductor Devices Division, Pilani, Rajasthan - 333031, India.
IEEE Log Number 8714152.

Experimental

SI GaAs substrates were used as a starting material. After standard cleaning, adhesion promoter (VM-651) was applied onto the substrate followed by coating of polyimide of different dilutions at different spin speeds. In our investigation, Dupont's 2550 polyimide was chosen due to its low-temperature baking cycle as compared to 2540 or 2545. Conventional photolithography steps involved the use of microposit 1350 J photoresist and its developer MF 312 followed by etching of polyimide in dilute solution of strong bases. Imidization conditions of polyimide film were varied and the etching behavior of the films were studied using SEM.

For planarization, windows of constant length and spacing of 10 μm each was first etched in 1.2 μm deposited silox film followed by polyimide coating under different deposition conditions. Talystep plots were used to determine the degree of planarization (ratio of step height after polyimide application to the initial step height of the oxide patterns).

Metal-insulator-metal structures were used for dielectric breakdown strength studies. Fully cured polyimide films were used as the insulator film. *I-V* characteristics obtained on a large number of capacitors were used to statistically determine the dielectric breakdown strength of polyimide films.

Results and Discussion

The etch rate and etch profile of the polyimide critically depends on the degree of imidization which, in turn, is a function of time and temperature. During the present investigation we observed that in the case of films with low imidization <35 percent, simultaneous control on the developing of positive resist and subse-